Arch. Metall. Mater. **69** (2024), 2, 493-496

DOI: https://doi.org/10.24425/amm.2024.149774

CHEOL-HUI RYU[1], YOUNG-IN LEE[1*]

SYNTHESIS OF MOLYBDENUM OXIDE NANOFIBERS WITH MULTIPLE SURFACE FACETS VIA ELECTROPSINNING FOLLOWED BY RAPID THERMAL TREATMENT

A MoO_3 nanofiber prepared by electrospinning and subsequent heat treatment is attracting significant attention due to its structural advantages. Vibrant studies are being conducted to control its morphology and diameter to improve its properties. In this study, we demonstrated the synthesis of α-MoO_3 nanofibers with multiple surface facets by controlling the heating rate and temperature in the heat treatment step for removing polymer and crystallizing MoO_3 from the electrospun polymer/precursor nanofibers. The analysis results show that the faster heating rate and higher heat treatment temperature in the thermal treatment process are more favorable for forming a shape in which particles with facet planes are connected. Finally, we observed the morphological change according to the heat treatment time to confirm the effect of the heat treatment conditions on the shape of MoO_3 and interpreted the results in terms of nucleation and crystal growth.

Keywords: MoO_3; nanofibers; surface facet; electrospinning; rapid thermal treatment

1. Introduction

Orthorhombic-phase α-MoO_3, which has an anisotropic crystal structure and variable oxidation states, is an attractive n-type semiconductor with many potential applications such as catalyst, gas sensor, photochromic and electrochromic devices, and rechargeable lithium-ion battery cathodes [1-4]. Since the performance of these applications is influenced by the structure of the material that affects its properties, research on synthesizing MoO_3 in various structures such as nanoplates, nanowires, nanobelts, nanotubes, and nanofibers is actively conducted [5-10].

Among various one-dimensional nanostructures, MoO_3 nanofibers prepared by an electrospinning process have a high aspect ratio and a controlled diameter and show a relatively large specific surface area through a microstructure composed of tiny nanosized grains and a porous nature [10-12]. Such a structure is advantageous for the applications above requiring chemical reactions. On the other hand, nanostructures composed of facets with high energy generally show greater reactivity because they have high surface energy. The MoO_3, which has remarkable crystallographic anisotropy, is being actively studied to improve its properties by synthesizing it into a structure with a facet of specific crystal planes [13-16].

After the first report on electrospun MoO_3 nanofibers by Sawicka et al. [17], some studies on the crystallinity, cation or anion doping, and diameter control of electrospun MoO_3 nanofibers have been reported. Gouma et al. [11] prepared MoO_3 nanowires with single-crystalline nature using electrospinning followed by a heat treatment for 10 h at 500°C. Li et al. [10] and Feng et al. [12] reported the electrospun MoO_3/Ce and MoO_3/C nanofiber to enhance the catalytic activity and electrochemical performance, respectively. Han et al. [16] synthesized ultra-long MoO_3 nanofibers with about 30 nm in diameter by optimizing the electrospinning process. However, α-MoO_3 nanofibers with multiple surface facets, which could show higher specific surface area and faster electron movement from the interior to the surface or vice versa, have yet to be previously reported.

Heat treatment is essential to synthesize oxide nanofibers because it removes the polymer used to make fibrous form and crystallizes the precursor into a metal oxide. In general, crystallization consists of nucleation and crystal growth steps, which can be controlled by the heat treatment temperature and the rate at which that temperature is reached. In this study, we attempted to synthesize α-MoO_3 nanofibers with multiple surface facets by controlling the heating rate to the temperature at which crystallization occurs. In addition, we studied in detail how the surface morphology of the samples prepared by electrospinning and heat treatment changes according to the heat treatment conditions.

[1] SEOUL NATIONAL UNIVERSITY OF SCIENCE AND TECHNOLOGY, DEPARTMENT OF MATERIALS SCIENCE AND ENGINEERING, SEOUL 01811, REPUBLIC OF KOREA

* Corresponding author: youngin@seoultech.ac.kr

2. Experimental

The viscous solution for the electrospinning was prepared by dissolving 0.5 g of polyvinyl pyrrolidone (PVP, Mw = 1,300 k, Sigma-Aldrich), 0.412 g of ammonium molybdate tetrahydrate [AM, $(NH_4)_6Mo_7O_{24} \cdot 4H_2O$, 99.98%, Sigma-Aldrich] and 0.174 g of citric acid in 9.1 g of mixture solvent with distilled water and ethanol. The transparent solution was loaded into a 10 ml plastic syringe with a nozzle and charged at 12 kV by a power supply to prepare the PVP/AM nanofibers. The electrospun products were collected at a metal collector with a fixed distance of 10 cm from the nozzle and dried at 60°C overnight. The heat treatment of the products was conducted at 500°C for 3 h in air with various heating rates of 3°C, 10°C, 20°C, and 25°C min^{-1} via rapid thermal process equipment (AccuThermo AW610, Allwin21 Corp., USA). In addition, the as-spun nanofibers were also thermally treated at 400°C and 500°C with a heating rate of 25°C min^{-1} for 10, 20, 50, 100, 200, and 500 min to confirm the morphology change during the heat treatment step. The crystal structures and morphology of the electrospun and heat-treated products were characterized by X-ray diffraction (XRD, X'Pert3 Powder, PANalytical, Netherlands) and field emission scanning electron microscopy (FE-SEM, S-4800, Hitachi, Japan).

3. Results and discussion

Fig. 1(a) shows representative FE-SEM images of electrospun PVP/AM products, indicating a smooth surface without any bead and a well-defined fibrous form. Their average diameter was about 430 nm, and their length could reach several micrometers. The crystalline phases of the products obtained by thermally treating the PVP/AM nanofibers at 500°C for 3 h using various heating rates were investigated by XRD, as shown in Fig. 1(b). All samples have the same diffraction peaks indexed to be orthorhombic a-MoO_3 structure (JCPDS card No. 35-0609), indicating that all products had no secondary phases. However, the peak intensities However, as summarized in TABLE 1, the intensity of specific peaks in each diffraction pattern was different for each sample. All samples show a higher ratio between the intensities of (040)/(110) and (040)/(021) diffraction peaks compared with those of standard reference in JCPDS, which is consistent with the preferred (010) facets. The (040)/(110) and (040)/(021) values increased as the heating rate slowed during the heat treatment of the PVP/AM nanofiber. It can be inferred that this is because the nucleation rate slows down at the slower heating rate, and the crystal growth from the nuclei increases, resulting in the prominent growth of the (040) plane. On the other hand, in the case of a fast-heating rate, the crystal growth is relatively tardy due to burst nucleation, which can be interpreted as a relatively small size of the (040) plane [18-19].

TABLE 1

Calculated intensity ratios between the (040)/(110) and (040)/(021) diffraction peaks in X-diffraction patterns in Fig. 1(b)

Samples	I(040)/I(110)	I(040)/I(021)
JCPDS (35-0609)	0.494	0.38
3°C/min	3.284	0.624
10°C/min	1.395	0.505
20°C/min	1.245	0.345
25°C/min	1.078	0.359

FE-SEM analysis shown in Fig. 2 was performed to confirm the effect of the heating rate on the shape of the heat-treated samples. By raising the temperature to 500°C at the slowest rate, the sample exhibited a complete plate shape, unlike the fibrous form of the electrospun PVP/AM sample, as shown in Fig. 1(a). Each plate shape particle was separated. As the heating rate to reach 500°C increases, it can be seen that the particle size is smaller than that of the plate-shaped particles observed in Fig. 2(a), and the facet plane is also observed, but it is elongated and round, unlike Fig. 2(a). This shape difference agrees with the XRD analysis results in Fig. 1(b) and TABLE 1. In addition, the particles were connected, and the number of connected particles increased as they were heated faster, resulting in a higher aspect ratio. As a result, a one-dimensional structure with multiple surface facets was obtained at the fastest heating rate.

To confirm the relationship between the final shape of the heat-treated MoO_3 sample and the heating rate and temperature, time-dependent experiments were conducted at 400°C and

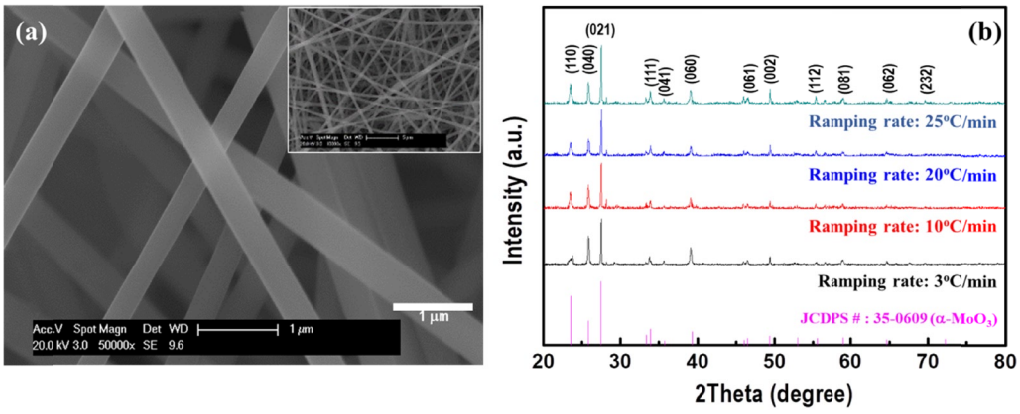

Fig. 1. (a) FE-SEM images of electrospun PVP/AM nanofibers and (b) XRD patterns of the products synthesized by an electrospinning process followed by a thermal treatment at 500°C for 3 h with different ramping rates; 3°C/min, 10°C/min, 20°C/min and 25°C/min

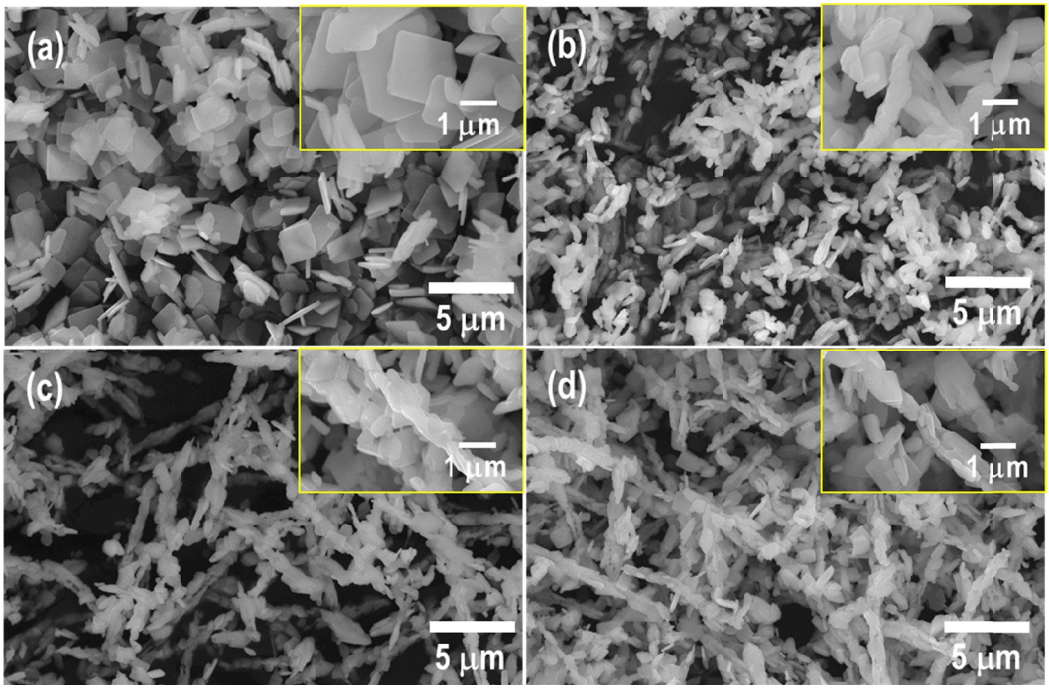

Fig. 2. FE-SEM images of the MoO_3 particles synthesized by an electrospinning process followed by a thermal treatment at 500°C for 3 h with different ramping rates; (a) 3°C/min, (b) 10°C/min, (c) 20°C/min and (d) 25°C/min

500°C, and the products were analyzed with FE-SEM. Fig. 3 shows FE-SEM images of the samples treated at 400°C for a specific holding time. It is difficult to observe any particular change until the holding time of 20 min. In the sample heat-treated for 50 min., a small number of MoO_3 plates similar to those shown in Fig. 2(a) were observed, and the fiber diameter began to decrease. Afterward, more MoO_3 plates were observed as the treatment time increased, and the fibrous shape disappeared. This shape change can be explained by the nucleation rate of MoO_3 occurring in the heat treatment step. Heat treatment at a relatively low temperature of 400°C slows down PVP decomposition in the electrospun PVP/AM nanofibers, thereby limiting the MoO_3 nuclei generated from AM. In general, crystal growth relatively lowers the surface energy contributing to the total free energy compared to nucleation [20]. Therefore, the growth of already generated nuclei occurs, and a plate shape is formed, as shown in Fig. 3(c) to (f).

Fig. 4 shows the morphological change of the sample thermally treated over time at 500°C, which could induce the nucleation of MoO_3 more quickly. Fig. 4(a) shows that many fine particles are formed on the surface of nanofibers from the heat treatment for 10 min., which can be explained as a result of the rapid nucleation of MoO_3. As observed from the heat-treated sample for 20 min., the formed nuclei grew into plate-like particles through subsequent crystal growth, but unlike the sample at 400°C, the size of the particles was relatively small, and the

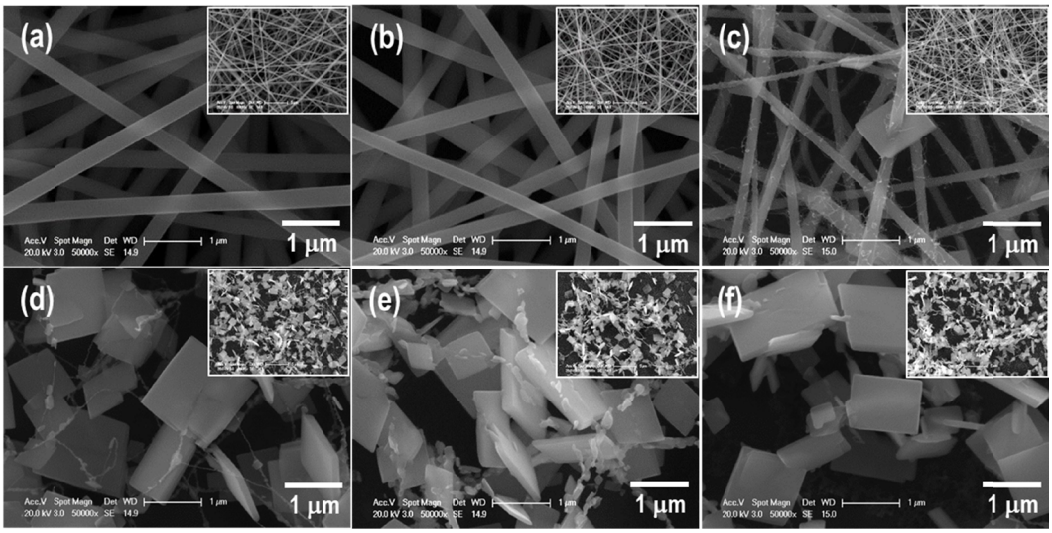

Fig. 3. FE-SEM images of the MoO_3 particles synthesized by an electrospinning process followed by a thermal treatment at 400°C with a ramping rate of 25°C/min for different time; (a) 10 min, (b) 20 min, (c) 50 min, (d) 100 min, (e) 200 min, and (f) 500 min

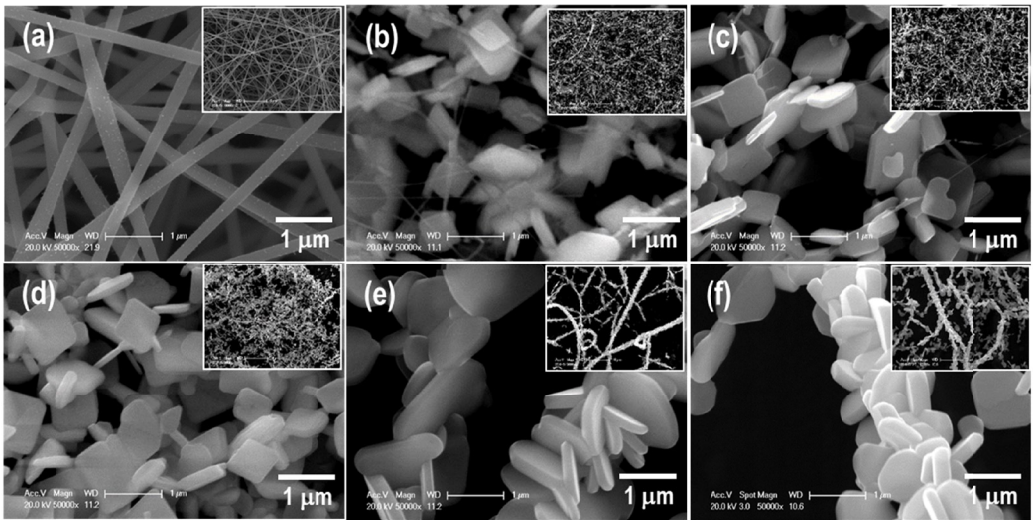

Fig. 4. FE-SEM images of the MoO_3 particles synthesized by an electrospinning process followed by a thermal treatment at 500°C with a ramping rate of 25°C/min for different time; (a) 10 min, (b) 20 min, (c) 50 min, (d) 100 min, (e) 200 min, and (f) 500 min

shape was elongated and round. The most important difference from the sample heat-treated at a relatively low temperature is that each particle is connected to the other and maintains a fibrous form, as shown in the inset pictures. The morphology is because a plurality of nuclei generated in the early stages grew adjacent and did not separate into individual particles. Therefore, it can be seen that the electrospun PVP/AM nanofibers were successfully transformed into MoO_3 nanofibers having multiple facets on the surface through a fast-heating rate and heat treatment at an appropriate level to promote rapid nucleation.

4. Conclusion

In summary, we have successfully synthesized the MoO_3 nanofibers with multiple facets on the surface using the electrospinning process followed by heat treatment with controlled temperature and heating rate. The XRD and FE-SEM analysis results show that the temperature and heating rate in the thermal treatment for removing PVP and crystallizing MoO_3 from the electrospun PVP/AM nanofibers can control the crystallographic characteristics and shape of the finally formed MoO_3. The faster heating rate and higher heat treatment temperature in the calcination process rapidly remove the PVP and induce burst nucleation of MoO_3 in the PVP/AM nanofibers. Therefore, each nucleus can grow adjacent, and the synthesized MoO_3 could have a fibrous shape with multiple facets on the surface. It is expected that the heat treatment process's temperature and heating rate control can be applied to other oxides with a crystal structure capable of facet growth to synthesize nanofibers with facets on the surface.

Acknowledgments

This study was supported by the Research Program funded by the SeoulTech (Seoul National University of Science and Technology).

REFERENCES

[1] R. Malik, N. Joshi, V.K. Tomer, Mater. Adv. **2**, 4190 (2021).
[2] A.V. Avani, E.I. Anila, Int. J. Hydrog. **47**, 20475 (2022).
[3] L. Zheng, Y. Xu, D. Jin, Y. Xie, Chem. Mater. **21**, 5681 (2009).
[4] S.R. Sahu, V.R. Rikka, P. Haridoss, A. Chatterjee, R. Gopalan, R. Prakash, Adv. Energy Mater. **10**, 2001627 (2020).
[5] Y. Liu, P. Feng, Z. Wang, X. Jiao, F. Akhtar, Sci. Rep. **7**, 1845 (2017).
[6] K.J. Samdani, D.W. Joh, M.K. Rath, K.T. Lee, Electrochim. Acta **252**, 268 (2017).
[7] S. Lee, N. Kwon, J. Roh, K.-J. Lee, J. Powder Mater. **27**, 394 (2020).
[8] M. Sajadi, M. Ranjbar, R. Rasuli, Appl. Surf. Sci. **527**, 146675 (2020).
[9] D.C. Look, Mater. Sci. Eng. B-Adv. Funct. Solid-State Mater. **80**, 383 (2001).
[10] W. Li, S. Zhao, B. Qi, Y. Du, X. Wang, M. Huo, Appl. Catal. B: Environ. **92**, 333 (2009).
[11] P. Gouma, K. Kalyanasundaram, A. Bishop, J. Mater. Res. **21**, 2907 (2006).
[12] C. Feng, H. Gao, C. Zhang, Z. Guo, H. Liu, Electrochim Acta, **93**, 101 (2013).
[13] F. Wang, W. Ueda, Chem. Eng. J. **15**, 742 (2009).
[14] P. Srinivasan, J.B.B. Rayappan, Microchim. Acta **186**, 797 (2019).
[15] J. Li, Y. Ye, L. Ye, F. Su, Z. Ma, J. Huang, H. Xie, D. E. Doronkin, A. Zimina, J.-D. Grunwaldt, Y. Zhou, J. Mater. Chem. C **7**, 2821 (2019).
[16] Y. Han, Y. Rheem, K.-H. Lee, H. Kim, N.V. Myung, J. Ind. Eng. Chem. **62**, 231 (2018).
[17] K.M. Sawicka, M. Karadge, P.-I. Gouma, Mater. Res. Soc. Symp. Proc. **847**, EE9.46.1 (2005).
[18] H. You, J. Fang, Nano Today. **11**, 145 (2016).
[19] W. Cui, X. Li, C. Xie, H. Zhuang, S. Zhou, J. Weng, Biomaterials **31**, 4620 (2010).
[20] N. T. K. Thanh, N. Maclean, S. Mahiddine, Chem. Rev. **114**, 7610 (2014).